

Slope stability assessment along Indian Himalayan National Highway NH-154A

Kanwarpreet Singh (✉ kanwarpreet.e9570@cumail.in)

Chandigarh University <https://orcid.org/0000-0002-7012-1815>

Research Article

Keywords: Slope stability, Factor of safety, Transport corridor, Chamba Himalaya

Posted Date: June 22nd, 2022

DOI: <https://doi.org/10.21203/rs.3.rs-1520452/v1>

License:   This work is licensed under a Creative Commons Attribution 4.0 International License.

[Read Full License](#)

Abstract

The road cut rock slope stability assessment along the Chamba-Bharmour road corridor of NH-154A has been carried out in present study based on the geological and geotechnical investigations as published In Journal Geological Society of India (Singh and Kumar 2020). The type of failure in the rock slopes has been identified using kinematic analysis based on Markland's test. The factor of safety (FOS) of identified planar and a wedge failures was evaluated using method proposed by Hoek and Bray. Extensive field work has been performed for collecting rock samples and to record input parameters like joint orientations for stereonet plotting. A total of six out of fourteen potentially unstable rock slopes at different locations along the NH-154A have been taken into consideration for their stability analysis. The unstable rock slope sections L3R1, L16R8, L19R14, L27R12, and L29R13 fulfill the criteria for plane failure conditions while L16R8, L25R10, L26R11, L27R12, L29R13 fulfill the criteria for wedge failure. It has been found that the FOS was identified to be less than one for planar failure at two sites while the minimum value of FOS for planar failure at other two sites falls between 1.0–1.2. The FOS of the plane failure at a single site was evaluated as greater than 2. The wedge failures identified at five sites had FOS greater than one. The site specific mitigation and control measures have been evolved for critical rock cut slopes.

1. Introduction

Downward movement of the slope forming materials under the influence of the gravitational forces often take place at the cut slopes along the highway stretches causes loss of life and property every year in hilly areas at global scale (Aleotti and Chowdhury 1999; Dikshit et al. 2020). The stabilized original and modified slopes are required for the constructional activities of the new transport corridors (Sharma et al. 2013). The road cut slope stability can get affected because of the improper methods applied for constructing and widening of the highway stretches in the mountainous regions (Singh et al. 2013; Sardana et al. 2019). Hence the geotechnical studies are important to understand the geological conditions before the construction of any project like dam, tunnel, and road etc. (Kainthola et al. 2013; Zheng et al. 2019). The major factors which influence the stability of the cut slopes are the shear strength parameters of the slope materials, orientation of discontinuities, and subsurface water conditions. The instability in the rocky terrain is the major geohazard in hilly areas (Pantelidis 2009, Shahri et al. 2019). It has become necessary to analyse and understand the slope stability approaches due to increase in the man made cuts because of the construction of various projects (Abramson et al. 2002; Bowa et al. 2019). It is a major problem for the geotechnicians to predict the slope stability which is crucial during design of tunnels, transport stretches, and dams (Li et al. 2008) which is creating attention of many researchers, designers, planners (Dong-pinga et al. 2016).

The intact rocks or the rock blocks are the major characteristics of rock slopes which are mainly due to the presence of discontinuities (Aqeel et al. 2014). The pre-existing discontinuities initiate failures in rock slopes rather than the breakage through intact rocks (Maerz et al. 2015). In some cases, the mechanism of the rock slope failure is difficult to analyze due to the presence of random joint sets. Based on the

geologic structure, any rock slope can be divided into main zones: a) discontinuity zone in which the rock sliding can be identified and analyzed, b) a revealing zone in which random set of discontinuities are present and thus a specific slope failure mechanism is difficult to identify and analyze (Maerz et al. 2012). A single rock, boulder, independently moving rocks in a small group may get dislodged from the original slope surface and fall downward under the gravitational force (Ansari 2015). The rock slope can fail in different modes of plane, wedge, and topple failures depending upon the orientation of discontinuities (Anbalagan et al. 1992; Kliche 1999). Therefore, there are various specific methods for detailed slope stability assessment for potential modes of failures. Based on the a) geometrical properties of exposed discontinuities and the slope, b) geometrical relationship between the orientation of discontinuities and slope, the potential modes of failures (planar, wedge, and topple) in rock slopes can be evaluated (Aqeel et al. 2018). To analyze the unstable discontinuous zones in rock slopes, various conventional methods i.e. kinematic analysis and limit equilibrium or numerical methods i.e. finite element method techniques can be utilized significantly. The kinematic analysis is currently being adopted worldwide (Olaleye and Ajibade 2011) which is simple and time saving approach to identify various potential modes of failures like planar, wedge, and topple in case of rock slopes (Markland 1972, Hoek and Bray 1981, Yoon et al. 2002).

Based on the Limit Equilibrium methods (LEM), the rock slope failure takes place over a discontinuity surface, when shear stresses become more than the shear strength of the slope forming rock. These approaches are made by the deterministic calculation of factor of safety (FOS) (Hoek 2007). However, numerous authors have adopted these methods for slope stability of the rock slopes, but this method has a limitation that the failure mode in the rock must be identified before these methods can be implemented. These methods cannot recognize the type of failure without the help from prior kinematic analysis (Kim et al. 2004).

There are various specific software packages based on simulation to analyze the slope instability (Guntel and Acar 2016; Topal et al. 2017; Yongsheng et al. 2019). In some cases, more than one type of failure may take place in the same rock slope for which more effort is required in terms of selecting different techniques to analyze instability. Numerous researchers have been adopted conventional rock mass classification, kinematic, and LEM approaches for slope stability assessment in Himalaya (Umrao et al. 2011; Singh et al. 2017; Trivedi et al. 2012; Pradhan et al. 2015; Siddique et al. 2015; Kundu et al. 2016; Sarkar et al. 2016; Chaurasia et al. 2017; Kumar et al. 2017) and advanced numerical simulation methods (Sarkar and Singh 2008; Umrao et al. 2017; Vishal et al. 2017).

District Chamba is a mountainous region through which many highway road corridors are traversing. Many settlements are built nearby or at the toe of these elevated areas. The major reason of frequent landsliding in the region is the man made cuts due to unplanned road construction in the numerous weak zones, mechanical excavation, and deficient blasting. Many rock failure events (Fig. 1) have been noticed along National Highway- 154A in district Chamba mainly during rainy season. The reconnaissance visits have been conducted to develop field based datasets of poorly excavated man made road cut rock

slopes having potential of failure. The FOS of critical rock slope sections was calculated by using Hoek and Bray (1981) method to suggest various mitigation measures to reduce life and property losses.

2 Materials And Method

2.1 Location and Geological settings

The study area lies along 62km long NH-154A in the Chamba district of Himachal Pradesh state (India) connecting district head quarters with Bharmour city and many other major settlements in the study area. The Chamba – Bharmour National Highway is located between 32°33'12.24"N, 76°7'32.88"E, and 32°26'34.08"N, 76°31'58.44"E (Fig. 1). The altitude in the region of Chamba varies from 2000 to 21,000ft. The major drainage source in the region is the river Ravi flowing along the highway which is a trans-boundary river passing through northwestern India and Pakistan. The monsoon season, however, is a predominant natural occurrence in the region because most of the rainfall takes place during monsoon season. The selected corridor passes along the banks of river Ravi from Bharmour town towards Chamba city. Various hydroelectricity projects, tourist spots, and famous Temples are there along the NH. The vegetation in the area is affected by the climatic conditions, lithology of the terrain, and soil types. The barren, sparsely and moderately vegetated slopes have been found along Chamba – Bharmour road section. Thickly vegetated forest land is also present at various places. The types of trees along the route are mostly the pines, while near Bharmour Township deodar trees are also there. The agriculture land in the study area is occupied by walnuts, kidney bean, chilly, and apple orchards.

The geology of the Chamba region is the combination of the wide range of the rock formations of age from late Proterozoic to Triassic (Rattan 1973; Sharma and Bholra 2004; Agarwal and Kumar 2004). In the Chamba region located on southwest side of the central crystalline zone, Batal Formation along with a basal unit of Manjir conglomerate overlies the Chamba Formation of Salkhala Group. The Salkhala Group is surrounded by the Vaikrita Group of central crystalline zone below, and Manjir - Batal (Katari Gali) formations in Chamba area. The broad classifications of Salkhala Group are Bhalai and Chamba Formations (Rattan 1973). Weathered rocky terrain is there in the field along the NH-154A. A clear exposure can be observed on cut slopes showing well developed discontinuities in the form of foliations and joints.

The rock exposures along the Chamba - Bharmour road belonging to Salkhala Group and Chamba Formation were identified as quartzites, slates, gneiss, and phyllites along with the quaternary deposits at some places on the left bank of the Ravi river. At few places the river born material (RBM) and conglomerates are also observed. Thin overburden also exists covering the rocks. The quartzites are mainly in the lower region of the study area in the Chamba and its nearby zone, while slate rocks exist in the upper region along the highway. The closely to widely spaced joints have been observed in case of the quartzite rocks along the Chamba – Bharmour road section. The well foliated joint surface has been observed as smooth and slightly rough. The quartzite rocks are slightly to moderately weathered and massive at various places. Mainly three sets of joints along with random joints have been exposed on the slopes at various places. Along the surface of the joints, weathering is more prominent. The joints are

well spaced with minimum and maximum spacing about few cm to more than 1m. The condition of the joints is open to moderately tight at various places. The ground water condition of the joints is mainly dry. The well foliated and jointed slates have shining dark grey colour as observed along the Chamba - Bharmour highway. The road cut slopes are mainly having moderately to the steep slopes along the NH. The joints have been observed to be dry, wet, and dripping ground water conditions on the exposed surfaces. Smooth to very rough joints are seen in the slates along with the cracks and the broken joints.

2.2 Slope stability assessment

In order to carry out the detailed stability analysis of the hazardous rock slopes, 1:1,000 scale has been selected which is also known as micro scale. The factor of safety (FOS) will also be evaluated for the selected rock slope sections.

2.2.1 Detailed slope stability assessment of rock slopes

The stability assessment of rock slopes depends upon the cohesiveness of the rock and various other geotechnical and structural parameters. The rock slope stability assessment for identified planar and wedge failures has been carried out in detail by employing a method as proposed in (Hoek and Bray 1981) for those rock slopes having plane and wedge failures.

2.2.1 Plane failure analysis

The FOS of the rock slope can be evaluated on the basis of the assumptions (Hoek and Bray 1981). Assumptions for plane failure analysis as shown in Fig. 2 are as listed below:

- The strike of the surface of sliding, tension crack, and slope must be parallel.
- There may be water inside the vertical tension crack up to the depth Z_w .
- The accumulation of the water may takes place at the base of the sliding surface because of the water entering into it due to tension crack, which can comes out to the atmospheric pressure where the dipping of the sliding surface is lesser than the slope surface.
- The forces are acting through the center of gravity which shows that the failure is because of sliding only except any rotational moment.
- The Mohr Coulomb criterion of failure has been adopted to compare cohesion (c) and friction(φ).

The FOS in this case is the ratio between the total slide resisting forces to the total slide mobilizing forces and this can be calculated on the basis of Eq. (1) (Hoek and Bray 1981).

$$F = \frac{c.A + (W.\cos \Psi_p - U - V.\sin \Psi_p)\tan\phi}{W.\sin\Psi_p + V.\cos\Psi_p} \quad (1)$$

Where,

Ψ_p = Dip of failure plane

A = Area

W = Weight of sliding block

U = Uplift force due to water pressure on the sliding surface

V = Force due to water pressure on the tension crack

$$A = (H - Z) \cdot \text{cosec } \Psi_p \quad (2)$$

$$U = \frac{1}{2} \gamma_w Z_w (H - Z) \text{cosec } \Psi_p \quad (3)$$

$$V = \frac{1}{2} \gamma_w Z_w^2 \quad (4)$$

When the tension crack is on the upper surface

$$W = (1/2) \gamma \cdot H^2 \{(1 - (Z/H)^2) \cot \Psi_p - \cot \Psi_f\} \quad (5)$$

When the tension crack is on the slope face

$$W = (1/2) \gamma \cdot H^2 \{(1 - (Z/H)^2) \cot \Psi_p \cdot (\cot \Psi_p - \tan \Psi_f)\} \quad (6)$$

2.2.2 Wedge failure analysis

Based on the general criterion to fulfill the occurrence of a wedge failure, the researchers Hoek and Bray (1981) have suggested a method to calculate factor of safety during wedge failure analysis. The basic mechanism of sliding in case of wedge failure is clearly shown in Fig. 3.

The above given geometry will be considered for analyzing the wedge failure. The hypothesis to be followed for water pressure distribution in case of the wedge failure depends upon the impermeability of the wedge itself. The water enters from the top of the wedge along intersection lines three and four and its leakage occur along the intersection lines one and two along the face of the slope as shown in Fig. 4.

The maximum water pressure will be along the line of intersection of 5 and is as shown in Fig. 5 and being zero along the lines 1, 2, 3, and 4. The failure of the wedge is along the line of intersection 5. These water conditions are assumed as the extreme conditions which can take place during the heavy rainfall.

The number wise pattern of the intersection lines followed for stereo net is shown in Fig. 6 in which line number 1 and 2 represent the intersections of plane A and B respectively with the slope face. The intersections of the plane B and A with the upper slope surface are represented by lines 3 and 4 respectively. The wedge failure is along the line of intersection 5 made by intersection of planes A and B. The FOS value in case of the wedge failure can be determined on the basis of Eq. (7) (Hoek and Bray 1981).

$$F = \left\{ \frac{3}{\gamma H} (C_A \cdot X + C_B \cdot Y) \right\} + \left\{ \left(A - \frac{\gamma_w}{2\gamma} \cdot X \right) \tan \phi_A + \left(B - \frac{\gamma_w}{2\gamma_r} \cdot Y \right) \tan \phi_B \right\} \quad (7)$$

Where,

C_A and C_B are the cohesive strengths of planes A and B

ϕ_A and ϕ_B are the angles of friction on planes A and B

γ is the density of the rock

γ_w is the density of the water

H is the total height of the wedge

X, Y, A and B are dimensionless factors which depend upon the geometry of the wedge, can be evaluated from the stereo plot as shown in Fig. 4.7.

$$X = \frac{\sin \theta_{24}}{\sin \theta_{45} \cdot \cos \theta_{2.na}} \quad (8)$$

$$Y = \frac{\sin \theta_{13}}{\sin \theta_{35} \cdot \cos \theta_{1.nb}} \quad (9)$$

$$A = \frac{\cos \Psi_a - \cos \Psi_b \cdot \cos \theta_{na.nb}}{\sin \Psi_5 \cdot \sin^2 \theta_{na.nb}} \quad (10)$$

$$B = \frac{\cos \Psi_b - \cos \Psi_a \cdot \cos \theta_{na.nb}}{\sin \Psi_5 \cdot \sin^2 \theta_{na.nb}} \quad (11)$$

Where

Ψ_a and Ψ_b are dipping angles of planes A and B respectively

Ψ_5 is the plunge of the line of intersection 5

X, Y, A and B are the dimensionless factors

3 Result

The detailed slope stability analysis of identified plane and wedge failures was carried out on a scale of 1:1,000, which is an appropriate scale for slope stability analysis. Finally, the factor of safety (FOS) has been evaluated for the rock using method proposed by Hoek and Bray 1981.

The stability assessment of rock slopes depends upon the physical strength of the rock and various other geotechnical and structural parameters. The unstable rock slope sections L3R1, L16R8, L19R14, L27R12, and L29R13 fulfill the criteria for plane failure conditions while L16R8, L25R10, L26R11, L27R12, L29R13 fulfill the criteria for wedge failure.

3.1 The plane failure analysis

Markland's test states that if $\psi_s > \psi_p > \varphi$, the possibility of the plane failure occurrence is higher. The location wise stereo-plots were prepared to identify plane failures as mentioned in the manuscript (NHENG-1094). The shear strength parameters of cohesion (c) and friction (φ) were assumed as suggested by researcher (Bieniawski 1979, 1989, 1993). A standard value of the unit weight of rock (γ) was taken from the available literature based on the type of rock. The factor of safety was determined using Eq. 1 using orientation of slope and discontinuity. The major joints, Foliation (F), and friction angle (φ) at selected rock slopes are given in Table 1.

Table 1
Orientation details at location L3R1, L16R8, L19R14, L27R12, L29R13

L3R1			L16R8		L19R14	
Sr. No.	Joints	Dip of Joints	Joints	Dip of Joints	Joints	Dip of Joints
1	Slope	85°/N280°	Slope	75°/N	Slope	85°/N280°
2	<i>J1</i>	50°/ N 270°	<i>J1</i>	30°/N160°	<i>J1</i>	60°/N260°
3	<i>J2</i>	42°/N130°	<i>J2</i>	70°/N280°	<i>J2</i>	40°/N80°
4	<i>F</i>	52°/N45°	<i>F</i>	50°/N5°	<i>F</i>	45°/N35°
5	ϕ	35°	ϕ	35°	ϕ	35°
L27R12			L29R13			
Sr. No.	Joints	Dip of Joints	Joints	Dip of Joints		
1	Slope	80°/N5°	Slope	60°/N30°		
2	<i>J1</i>	60°/N25°	<i>J1</i>	70°/N220°		
3	<i>J2</i>	71°/N275°	<i>J2</i>	56°/N315°		
4	<i>F</i>	40°/N10°	<i>F</i>	45°/N40°		
5	ϕ	35°	ϕ	30°		

Slope section L3R1

This rock slope section is the first location on NH-154A from Chamba town towards Bharmour and is located at about 500m upstream of NHPC Power House. It has been observed that at location L3R1, hard, massive, moderately weathered, and fairly jointed quartzite is exposed at the cut slope. Many of the joint surfaces show iron stain as well as other encrustations. The dirty colored quartzites are medium to fine-grained with moderately developed joints. The height of the slope is about 28-30m. The major joints (and) observed on the slope, Foliation , and friction angle are given in Table 1. The upper slope at the site is sparsely vegetated. The slope has been found unstable because the joint encounters a plane failure, hence the plane failure analysis has been performed at slope section L3R1. The factor of safety of the slope has been determined for the dry condition when the depth of water in the tension crack is zero, and for the wet condition when the $\gamma_w = \gamma_{sat} - \gamma_{water}$, and utilizing the input parameters as given in Table 2. The factor of safety value has been determined as 1.7 for dry slope and 1.0 for the wet slope condition. The similar procedure as given in Table 2 for calculation of FOS is adopted for other locations where plane failure has been identified.

Slope section L16R8

This rock slope is located near Bahog village along NH-154A at distance of 1km from Lothal. This slope has height and length about 35 and 15m respectively and is inclined at an angle 75° towards the north. A sparsely vegetated area has been observed on the upper slope. The attitude of the slope is controlled by the disposition of the foliation planes at location L16R8 where the foliation planes dip toward the valley at an angle less than the slope as given in Table 1. At this site, the mode of failure was plane because of . The foliation dips at an angle less than the slope angle and its direction is nearly parallel to the slope i.e. within 20° of the slope angle. In addition, the wedge was also observed due to the intersection of and , and the direction of the plunge which is nearly parallel to the slope direction. The FOS of the current slope has been evaluated as 1.5 and 1.2 for dry as well as wet slope conditions by following the same procedure as mentioned in Table 2. The factor of safety showed that the slope is stable during the dry as well as wet conditions.

Table 2
FOS calculation for slope section L3R1

Slope condition`	Input parameters	Functions calculated	Calculations using formula	FOS
For dry condition	$\psi_p = 50^\circ$	$\text{Cosec } \psi_p = 1.305$	$A = (H - Z) \cdot \text{cosec } \psi_p = 12.64\text{m}^2$	1.7
	$\psi_f = 85^\circ$	$\text{Cot } \psi_p = 0.839$	$U = \frac{1}{2} \gamma_w Z_w \cdot (H - Z) \cdot \text{cosec } \psi_p = 0\text{t/m}$	
	$\gamma = 2.6 \text{ t/m}^3$	$\text{Cot } \psi_f = 0.087$	$V = \frac{1}{2} \gamma_w \cdot Z_w^2 = 0\text{t/m}$	
	$\gamma_w = 1 \text{ t/m}^3$	$\text{Sin } \psi_p = 0.766$	$W = \frac{1}{2} \gamma H^2 \left\{ \left(1 - \frac{Z^2}{H} \right) \cot \psi_p - \cot \psi_f \right\}$ $= 429.29\text{t}$	
	$Z_w = 0\text{m}$	$\text{Tan } \psi_f = 11.430$		
	$C = 30 \text{ t/m}^2$	$\text{Tan } \psi_p = 1.192$		
	$\varphi = 35^\circ$	$\frac{1}{2\gamma} \cdot H^2 = 1170.0$		
	$Z = 20.3\text{m}$	$\frac{Z}{H} = 0.677$		
	$H = 30\text{m}$	$1 - \left(\frac{Z}{H}\right)^2 = 0.542$		
For wet condition	$Z_w = 20.3\text{m}$		$U = 128.43 \text{ t/m}$	1.0
$(Z_w = Z)$			$V = 206.30\text{t/m}$	

Slope section L19R14

A nearly vertical slope (angle 85°) has been identified at location L19R14. This slope is 15m high and 10m in length. Moderately massive slates, which are well foliated and jointed, are exposed on this slope surface. The directions of the discontinuities and the slope at the selected section are given in Table 1. From the stereo-net, it has been observed that $J1$ is a potential joint for plane failure. The direction of the joint set $J1$ is within 20° of the slope direction and its inclination is lesser than the slope, hence the conditions for the plane failure exist. The FOS value was determined as 1.8 for dry slope and 0.89 for wet slope, which shows that the slope is stable during the dry condition while, it becomes unstable at wet conditions.

Slope section L27R12

This rock slope site is located at a distance of 2.5km from village Luna towards the Chamba Township. Grey colored, well-foliated slates are exposed at this cut slope. The cut slope is 40m high and 20m in length and is inclined at an angle 80° . The joints are tight with some of them having good strike condition. The direction of the slope and discontinuities measured are given in Table 1. The discontinuities observed at the site were plotted in the stereo net corresponding to the friction circle of 35° . The joints intersection and joints indicated that the plane failure occurred due to F and $J1$ planes, because they dip at an angle less than that of the slope and more than ϕ . Also a wedge failure formed due to the line of intersection between $J2$ and F , $J1$ and $J2$. The plane failure based slope stability analysis was performed for the foliation F and the joint $J1$. As can be noted from the Table 1, for the plane failure along foliation, the FOS value is 1.4 in case of the dry slope, whereas the slope becomes unstable with 0.98 value of FOS for wet slope conditions. Hence, the rainfall activities may initiate the plane failure along the foliation at this section, when tension crack will get filled with water. For plane failure along $J1$, the factor of safety is 1.3 for dry slope, and 1.0 for wet slope condition. Hence, along both F and $J1$, the slope may become unstable due to the chances of plane failure during wet slope conditions.

Slope section L29R13

Moderate, dense, and grey colored slates are exposed at this cut slope which is 35m in height. The foliations are well developed at fairly closer spacing. The properties of the geological discontinuities at this site are given in Table 1. The foliation F , within the unstable zone, dips at an angle less than the slope; hence, it fulfills the conditions of the plane failure to occur at the slope section. In addition, the intersection of F and $J2$ forms a potentially unstable wedge. The factor of safety of the slope under the dry conditions has been evaluated as 2.3, and for wet slope conditions as 2.1.

3.2 The wedge failure analysis

The wedge failure analysis based detailed slope stability assessment was performed to determine the factor of safety at locations L16R8, L25R10, L26R11, L27R12, L29R13. The methodology adopted for evaluating the required inputs to calculate FOS for analyzing a wedge is given in methodology and data acquisition section. Based on the direction and the inclination of the slope and discontinuities, geometry of the wedge was plotted manually on the stereo plot to determine the dimensionless factors of A , B , X , and Y values. The factor of safety of the wedge failure was determined from Eq. 7.

Where,

C_A and C_B are the cohesive strengths of planes A and B

φ_A and φ_B are the angles of friction on plane A and B

γ is the density of the rock

γ_w is the density of the water

H is the total height of the wedge

Slope section L16R8

The slope section L16R8 is composed of light grey, hard, and massive slate rock. The surface of the slope is rough and slightly weathered. The cut slope is inclined at an angle 75° towards N. The inclination of the upper slope is about $N20^\circ$. Traversing of many joints was noticed on the rock surface. A cluster of three sets of joints was observed at the cut slope. The required inputs for defining the geometry of wedge based on the orientations of the slope, and discontinuities are given in Table 3. The line of intersection made by the discontinuities F and $J2$ has plunge and trend of 48° and $N344^\circ$ respectively. The factor of safety has been evaluated to be 2.7 (Table 4). Similar steps as given in the current Table were adopted to evaluate FOS for other rock slope sections, where wedge failure is identified.

Slope section L25R10

This rock slope site is located at a distance of 1km from village Gehra towards Bharmour. Grey colored, fine-grained, and hard massive slates, well traversed by foliations and joints, were exposed in this cut slope. This dry and unweathered cut slope is 38m high and 8m in length and is inclined at an angle 75° . The surface of the slope shows the effect of deficient blasting done in the past. The parameters for defining the wedge geometry are given in Table 3. The line of intersection made by discontinuities F and $J1$ has plunge and trend of 44° and $N359^\circ$ respectively. The factor of safety of the slope has been found to be 3.8.

Table 3
Orientation details at location L16R8, L25R10, L26R11, L27R12, L29R13

L16R8			L25R10			L26R11		
Plane	Dip	Dip direction	Plane	Dip	Dip direction	Plane	Dip	Dip direction
A	50°	N5°	A	50°	N35°	A	46°	N275°
B	70°	N280°	B	70°	N290°	B	72°	N55°
Slope	75°	N	Slope	75°	N350°	Slope	85°	N355°
Upper surface	20°	N	Upper surface	24°	N350°	Upper surface	6°	N355°
L27R12			L29R13					
Plane	Dip	Dip direction	Plane	Dip	Dip direction			
A	40°	N10°	A	45°	N40°			
B	71°	N275°	B	56°	N315°			
Slope	80°	N5°	Slope	60°	N30°			
Upper surface	20°	N5°	Upper surface	20°	N30°			

Slope section L26R11

Moderately massive, grey colored, and dense slates with well - developed joints and foliations are exposed at this slope. The cut slope is 39m high and 20m in length and is inclined at an angle 85°. The parameters for defining the wedge geometry are as given in Table 3. The line of intersection made by discontinuities F and $J1$ has plunge and trend of 27° and N335° respectively. The FOS of the slope was determined as 3.86.

Slope section L27R12

Rough and slightly weathered cut slope section L27R12 is 40m high and is inclined at an angle of 80°. The parameters for defining the wedge geometry are given in Table 3. The line of intersection made by discontinuities F and $J2$ has plunge and trend of 38° and N350° respectively. A wedge failure is also observed in case of the line of intersection formed due to F and $J1$, but the trend of the line of intersection does not lie within 20° of the slope direction, hence the conditions for wedge failure analysis are not fulfilled. The factor of safety was determined to be 2.8.

Slope section L29R13

This rough and slightly weathered cut slope is 35m high, and is inclined at 60°. The parameters for defining the wedge geometry are given in Table 3. The line of intersection made by discontinuities of F and $J2$ has plunge and trend of 40° and N10° respectively. The factor of safety of the slope was determined as 3.31.

Table 4
Wedge stability calculation sheet for location L16R8

Input data	Function value	Calculated values
$\psi_A = 50^\circ$	$\cos \psi_A = 0.643$	$A = \frac{\cos \psi_a - \cos \psi_b \cdot \cos \theta_{na.nb}}{\sin \psi_5 \cdot \sin^2 \theta_{na.nb}} = 0.80$
$\psi_B = 70^\circ$	$\cos \psi_B = 0.342$	$B = \frac{\cos \psi_b - \cos \psi_a \cdot \cos \theta_{na.nb}}{\sin \psi_5 \cdot \sin^2 \theta_{na.nb}} = 0.213$
$\psi_5 = 48^\circ$	$\sin \psi_5 = 0.743$	
$\psi_{na.nb} = 72^\circ$	$\cos \psi_{na.nb} = 0.309$ $\sin \psi_{na.nb} = 0.951$	$X = \frac{\sin \theta_{24}}{\sin \theta_{45} \cdot \cos \theta_{2.na}} = 3.826$
$\theta_{24} = 57^\circ$	$\sin \theta_{24} = 0.839$	
$\theta_{45} = 30^\circ$	$\sin \theta_{45} = 0.500$	$Y = \frac{\sin \theta_{13}}{\sin \theta_{35} \cdot \cos \theta_{1.nb}} = 0.280$
$\theta_{2.na} = 64^\circ$	$\cos \theta_{2.na} = 0.438$	
$\theta_{13} = 165^\circ$	$\sin \theta_{13} = 0.259$	$C_A \cdot X + C_B \cdot Y = 82.13$
$\theta_{35} = 74^\circ$	$\sin \theta_{35} = 0.961$	
$\theta_{1.nb} = 16^\circ$	$\cos \theta_{1.nb} = 0.961$	$(A - \frac{\gamma_w}{2\gamma_r} \cdot X) \tan \varphi_A = 0.063$
$\varphi_A = 35^\circ$	$\tan \varphi_A = 0.700$	
$\varphi_B = 35^\circ$	$\tan \varphi_B = 0.700$	$(B - \frac{\gamma_w}{2\gamma_r} \cdot Y) \tan \varphi_B = 0.113$
$\gamma_r = 2.7 \text{ t/m}^3$	$\frac{\gamma_w}{2\gamma_r} = 0.185$	
$\gamma_w = 1 \text{ t/m}^3$		
$C_A = 20 \text{ t/m}^2$		$\text{FOS} = \left\{ \frac{3}{\gamma H} (C_A \cdot X + C_B \cdot Y) \right\} + \left\{ \left(A - \frac{\gamma_w}{2\gamma_r} \cdot X \right) \tan \varphi_A + \left(B - \frac{\gamma_w}{2\gamma_r} \cdot Y \right) \tan \varphi_B \right\}$
$C_B = 20 \text{ t/m}^2$		
$H = 35 \text{ m}$		$\text{FOS} = 2.7$

4 Discussion

The detailed stability assessment of critical rock slopes in the area was done to identify the vulnerable slopes. The slopes (L3R1, L19R14, L25R10, L26R11, L16R8, L27R12, and L29R13), which were found to have either planer and/or wedge failures, were studied in detail for determining FOS. The slope site L3R1 with planer failure just stable with FOS's values 1.7 at dry and 1.0 at wet conditions while the slope site L19R14 with planar failure had FOS less than one at wet condition. Hence, it can be considered as unsafe. The sites (L25R10 and L26R11) showed wedge failure, and the FOS of these sites was found to be more than one. Hence, these sites can be considered as safe. For the remaining 3 sites (L16R8, L27R12, and L29R13), which showed both planer and wedge failures, the FOS values are greater than one at sites (L16R8 and L29R13), and hence, these can be considered as safe, while the FOS of slope section L27R12 was found to be less than one, and hence unstable.

After identifying the unstable slopes, it is essential to adopt suitable control measures to reduce the driving forces. So mitigation measures for the risk reduction become necessary to lessen the severity of landslide disasters with acceptable maintenance using minimum expenditure. The purpose of the present work is to assist decision making and to guide the users in the choice of the most appropriate control/mitigation measures for the potential landslide sites along the selected NH-154A highway corridor. The proposed mitigation measures are based on recommended practices, expert judgment, technology and experience. The terrain conditions, slope forming materials, and slope stability analysis conducted were considered for the proposed mitigation measures for unstable slopes.

The mitigation measures for rock slope sections along NH-154A have been suggested for improving their stability as per (Romana 1985; BIS 1997). The proposed reinforcement arrangements (Figure 7) for the identified rock slopes with plane and wedge failures are based on the methods proposed by researchers (Anbalagan et al. 2007; IRC 1998) etc.

L3R1

This rock slope section is located at about 500m upstream of NHPC Power House. The rock slope site has been observed to be affected by deficient blasting. Along the cut slope, open and loose joints are present on the cut slope surface, which is about 30m. The inclination of the slope is nearly vertical. The stability analysis indicates unstable condition mainly because of deficient blasting which had resulted in inducing additional open joints in the cut slope. Though, the overall slope is stable as indicated by FOS which is 1.7 and 1.0 at dry and wet conditions respectively, it is prone to failure locally due to steep slope and presence of open joints. Hence, its re-profiling at an angle of 60° is proposed as suggested by researcher (Romana 1985) and the mitigation measures were suggested based as per IRC 1998). The re-profiling of the slope surface results into its flattening which makes it less susceptible to sliding. Selective rock anchors should be further applied on the slope surface since the joint and dip into the hill, and the joint is nearly parallel but dipping at a low angle than the slope. The rock anchors should be installed nearly perpendicular to to strengthen and reinforce the unstable blocks or beds of rocks. The prevention of the loose rock blocks from their dislodging can be done by anchoring them into fresh rocks in case of

planar slides, major toppling and general slope instabilities. For anchoring, along block size 1.5 to 2m, anchor of length 5m should be applied at the spacing of 2 to 2.5m as shown in Figure 7 (a, b).

The steel bars of diameter 25 to 40mm can be used. The anchor plates of size 30×30cm should be fixed on top of the rock bolt. After rock bolting, a polymer wire mesh or net should be anchored on the slope surface with nails before shotcreting to prevent falling of loose rock and shotcrete pieces (Figure 7c). Then, the systematic shotcreting in the form of cement water slurry should be injected into it under high pressure of 0.5 to 1.0 kg/cm² to protect the slope surface from erosion and weathering. Shotcrete consist of water cement mortar and it can be applied to the slope surface by an air jet Figure 7(c, d). Thickness of the shotcreted layer varies from 50mm to 70mm. The shotcreting is mainly for highly jointed rocks and is profitable, which can be done very quickly.

L16R8

This rock slope site is located near Bahog village at a distance of 1km from village Lothal towards Bharmour city. On an average, the height of the slope is 35m. Along the cut slope, open and loose joints are present on the cut slope surface. The inclination of the slope is nearly vertical (75°). The stability analysis using SMR indicates completely unstable condition mainly because of the mechanical blasting which had resulted in inducing additional open joints in the cut slope. Though, the overall slope is stable as indicated by FOS in case of planar (FOS- Dry: 1.5, Wet: 1.2) and wedge (FOS: 2.7) failure analysis, it is prone to failure locally due to steep slope and presence of open joints. Hence, its re-profiling at an angle of 60° is proposed. Selective grout anchors should be provided to a depth of 5m in selected locations, where open joints are present.

L25R10

This rock slope is located at a distance of 1km from Gehra towards Bharmour. On an average, the height of the slope is about 38m. The slope is inclined at an angle of 75° towards N350°. Along the cut slope, open and loose joints are present on the cut slope surface. The stability analysis using SMR indicates unstable condition mainly because of the deficient blasting which had resulted in inducing additional open joints in the cut slope. Though, the overall slope is stable as indicated by FOS 3.8, it is prone to failure locally due to steep slope and presence of open joints. Since the slope angle is about 75°, anytime rock fragments may fall due to gravity action. Hence, the pruning of the slope to 60° has been proposed. Rock bolts should be applied at an angle perpendicular to and causing wedge failure. The shotcreting at the entire slope surface may be done to protect the slope surface from erosion and weathering. The polymer wire mesh will further prevent the free fall of rock and shotcrete pieces.

L27R12

This rock slope section is located at a distance about 2.5km from village Luna toward Chamba Township along NH-154A. The slope site is inclined at 80° towards N5°. On an average, the height of the slope is about 40m. The stability analysis using SMR indicates completely unstable condition mainly because of

the mechanical blasting. The slope is unstable as indicated by FOS 0.98, hence, it is prone to failure. Since the slope angle is about 80° , anytime rock fragments may fall due to gravity action. Hence, the pruning of the slope to 60° has been proposed. Rock anchoring should be applied on the rock surface since the discontinuities and are dipping nearly parallel at a lower angle than the slope. Since, a wedge is also formed at this slope section due to and , hence, the rock anchoring would be better option when applied at an angle perpendicular to the and . The shotcreting at the entire slope surface may be done to protect the slope surface from erosion and weathering. The critical open joints observed on the exposed rock surface may be protected by providing polymer wire mesh to prevent the free fall of rock and shotcrete pieces.

L19R14

A nearly vertical slope (85°) has been observed at location L19R14. On an average, the height of the slope is about 20m. The stability analysis using SMR indicates unstable condition mainly because of the deficient blasting. The slope is unstable as indicated by FOS 0.89, hence, it is prone to failure. Since the slope angle is about 85° , anytime rock fragments may fall due to gravity action. Hence, the pruning of the slope to 60° has been proposed. Rock anchoring should be applied on the rock surface since is dipping nearly parallel at a lower angle than the slope. The shotcreting at the entire slope surface may be done to protect the slope surface from erosion and weathering. The polymer wire mesh will further prevent the free fall of rock and shotcrete pieces.

L29R13

This slope site is located near Luna along NH-154A. The slope is inclined at 60° towards N 30° . On an average, the height of the slope is about 35m. A stable wedge has been identified at the rock slope section of L29R13 due to and . Since, the slope inclination is 60° , hence, re-profiling of the slope is not needed. No detailed mitigation measure is required at this slope surface. Hence, only a polymer wire mesh is required to cover the entire slope surface to prevent the free fall of rock pieces.

5 Conclusion

The detailed slope stability analysis of the 7 rock slopes has been performed in the present study. The rock slope stability assessment in detail has been carried out by employing a method proposed by Hoek and Bray for those rock slopes having planar and wedge failures which fall in SMR class (i.e. class IV and V). The FOS was identified to be less than one for two planar failures while it has been evaluated as more than one for the remaining planar and wedge modes of failures. The mitigation measures have been suggested for the hazardous rock slopes to ensure the safety of the traffic along the road section. The rock slopes which are completely unstable have been recommended to be first re-excavated, and then anchoring along with polymer wire mesh which will then be followed by shotcreting was suggested. The rock anchoring at other unstable rock slopes in a direction perpendicular to the potentially unstable joints causing planar and wedge failure was suggested followed by implementation of the polymer wire mesh and shotcreting.

Declarations

Authors are not having any financial or non-financial interests that are directly or indirectly related to the work submitted for publication

References

1. Abramson LW, Lee TS, Sharma S, Boyce GM (2002) Slope stability and stabilization methods, 2nd edn. Wiley, New York
2. Agarwal GS, Kumar B (2004) Status of Chamba formation, Chamba district, H.P, Rec. Geol. Surv. India, vol.136, pt.8, pp.111–113
3. Aleotti P, Chowdhury R (1999) Landslide hazard assessment: summary review and new perspectives. Bull Eng Geol Environ, (1999) 58(1):21–44. doi:10.1007/s100640050066
4. Anbalagan R, Sharma S, Raghuvanshi TK (1992) Rock mass stability evaluation using modified SMR approach. In: Proceedings of 6th natural symposium on rock mechanics, Bangalore, India, pp 258–268
5. Anbalagan R, Singh B, Chakraborty D, Kohli A (2007) A Field Manual for Landslide Investigations. Department of Science and Technology, New Delhi, India
6. Ansari MK, Ahmed M, Singh T, Ghalayani I (2015) Rainfall, a major cause for rockfall hazard along the roadways, highways and railways on hilly terrains in India. Eng Geol Soc Territ 1:457–460
7. Aqeel A, Maerz N, Anderson N (2014) Mapping subvertical discontinuities in rock cuts using a 400 MHz ground penetrating radar antenna. Arab J Geosci 7(5):093–2105
8. Aqeel A, Zaman H, Ahmed Abd EA (2018) Slope Stability Analysis of a Rock Cut in a Residential Area, Madinah, Saudi Arabia: A Case Study. Geotech Geol Eng. <https://doi.org/10.1007/s10706-018-0720-7>
9. Bieniawski ZT (1979) The Geomechanics Classification in rock engineering applications, In Proc. 4th Int. Congr. Rock Mech: Montreux, Chap. 5: Balkema, Rotterdam, pp. 55–95
10. Bieniawski ZT (1989) Engineering Rock Mass Classification. Wiley- Interscience, New York, p 251
11. Bieniawski ZT (1993) In: Hudson JA (ed) Classification of rock masses for engineering: The RMR system and future trends, comprehensive rock engineering, vol 3. Pergamon Press, New York, pp 553–574
12. Bowa VM (2019) Wedge Sliding Analysis of the Rock Slope Subjected to Uplift Forces and Surcharge Loads Conditions. <https://doi.org/10.1007/s10706-019-01027-4>. Geotech Geol Eng
13. Chaurasia AK, Pandey HK, Nainwal HC, Singh J, Tiwari SK (2017) Stability analysis of rock slopes along Gangadarshan, Pauri, Garhwal, Uttarakhand. J Geol Soc India 89(6):617–740
14. Dikshit A, Satyam N, Pradhan B, Sai K (2020) Estimating rainfall threshold and temporal probability for landslide occurrences in Darjeeling Himalayas, Geosciences Journal,

15. Dong-Pinga D, Lianga L, Jian-Fengb W, Lian-Henga Z (2016) Limit equilibrium method for rock slope stability analysis by using the Generalized Hoek-Brown criterion. *Int J Rock Mech Min Sci* 89:176–184
16. Guntel B, Acar A (2016) Rockfall modelling with remedial design and measures along part of a mountainous settlement area, southern Turkey. In: IOP conference series: earth and environmental science, vol 44, 022013
17. Han Z, Su B, Li Y, Ma Y, Wang W, Chen G (2019) Comprehensive analysis of landslide stability and related countermeasures: a case study of the Lanmuxi landslide in China, *JO - Scientific Reports*, 9, Article number: 9. 12407. <https://doi.org/10.1038/s41598-019-48934-3>. 1
18. Hoek E (2007) *Practical Rock Engineering*. Rocscience-Hoeks Corner. (2019), USA.2
19. Hoek E, Bray JW (1981) *Rock Slope Engineering*. Institution of Mining and Metallurgy, London, p 67
20. IRC: SP: 48 (1998) *Hill Road Manual*, The Indian Road Congress, New Delhi
21. IS. 13365 (1997) *Determination of Slope Mass Rating, Part 3* Bureau of Indian Standards, New Delhi
22. Kainthola A, Verma D, Singh TN (2013) Probabilistic and sensitivity investigation for the hill slopes in Uttarakhand, Lesser Himalaya, India. *Am J Numer Anal* 1(1):8–14
23. Kim KS, Park HJ, Lee S, Woo I (2004) Geographic Information System (GIS) based stability analysis of rock cut slope. *Geosci J* 8(4):391–4003
24. Kliche CA (1999) *Rock slope stability*. Society for Mining, Metallurgy and Exploration, London
25. Kumar S, Kumar K, Dogra NN (2017) Rock mass classification and assessment of stability of critical slopes on national highway-22 in Himachal Pradesh. *J Geol Soc India* 89(4):407–412
26. Kundu J, Mahanta B, Tripathy A, Sarkar K, Singh TN (2016) Stability evaluation of jointed rock slope with curved face, *INDOROCK 2016: 6th Indian rock conference 17–18 June 2016*. Indian Institute of Technology Bombay, Mumbai
27. Li AJ, Merifield RS, Lyamin AY (2008) Stability charts for rock slopes based on the Hoek–Brown failure criterion. *Int J Rock Mech Min Sci* 45(5):689–700
28. Li Y, Jiao Q, Hu X, Li Z, Li B, Zhang J, Jiang W, Luo Y, Li Q, Ba R (2020) Detecting the slope movement after the 2018 Baige Landslides based on ground-based and space-borne radar observations. *Int J Appl Earth Observation Geoinf Volume* 84:101949
29. Maerz N, Aqeel A, Anderson N (2015) Measuring orientations of individual hidden sub-vertical discontinuities in sandstone rock cuts integrating ground penetrating radar and terrestrial LIDAR. *Environ Eng Geosci* XXI(4):293–309
30. Maerz N, Youssef A, Otoo J, Kassebaum T, Duan Y (2012) A simple method for measuring discontinuity orientations from terrestrial Lidar images. *Environ Eng Geosci* 19(2):185–195
31. Markland JT (1972) A useful technique for estimating the stability of rock slopes when the rigid wedge sliding type of failure is expected. *Imp. Coll. Rock Mech. Res. Rep.* (1972), 19.2345

32. Olaleye BM, Ajibade ZF (2011) Kinematic analyses of different types of rock slope failures in a typical limestone quarry in Nigeria. *J Emerg Trends Eng Appl Sci* 2(6):914–920
33. Pantelidis L (2009) Rock slope stability assessment through rock mass classification systems. *Int J Rock Mech Min Sci* 46(2):315–325
34. Pradhan SP, Vishal V, Singh TN (2015) Study of slopes along river Teesta in Darjeeling Himalayan region. *Eng Geol Soc Territ* 1:517–520
35. Rattan SS (1973) Stratigraphy and sedimentation of Chamba area, Western Himachal Pradesh, *Him. Geology*, (1973), vol. 3, pp. 231–248
36. Romana M (1985) New adjustment ratings for application of Bieniawski classification to slopes. *Proceedings of the International Symposium on the Role of Rock Mechanics in Excavations for Mining and Civil Works*, ISRM, vol. 195, pp. 49–53
37. Sardana S, Verma AK, Verma R et al (2019) Rock slope stability along road cut of Kulikawn to Saikhamakawn of Aizawl, Mizoram, India. *Nat Hazards*. <https://doi.org/10.1007/s11069-019-03772-4>
38. Sarkar K, Singh TN (2008) Slope stability study of himalayan rock—a numerical approach. *Int J Earth Sci Eng* 1:7–16
39. Sarkar K, Singh AK, Niyogi A, Behera K, Verma AK, Singh TN (2016) The assessment of slope stability along NH-22 in Rampur-Jhakri area, Himachal Pradesh. *J Geol Soc India* 88:387–393
40. Shahri AA, Spross J, Johansson F, Larsson S (2019) Landslide susceptibility hazard map in southwest Sweden using artificial neural network, *Catena*, Volume 183, 2019, 104225, ISSN 0341–8162, <https://doi.org/10.1016/j.catena.2019.104225>
41. Sharma BK, Bhola AM (2004) Microstructures of co-axially folded vein segments and crenulation cleavage: Evidence for dissolution phenomena in the Chamba thrust sheet. *Western Himalayas, Episodes*. (in press)
42. Sharma RK, Mehta BS, Jamwal CS (2013) Cut slope stability evaluation of NH-21 along Natayan – Gambhrola section, Bilaspur district, Himachal Pradesh, India. *Nat Hazards* 66:249–270. [doi:10.1007/s11069-012-0469-x](https://doi.org/10.1007/s11069-012-0469-x)
43. Siddique T, Alam MM, Mondal MEA, Vishal V (2015) Slope mass rating and kinematic analysis of slopes along National Highway-58, near Jonk, Rishikesh, India. *J Rock Mech Geotech Eng* 7:600–606
44. Singh K, Kumar V (2021) Slope stability analysis of landslide zones in the part of Himalaya, Chamba, Himachal Pradesh, India. *Environ Earth Sci* 80:332. <https://doi.org/10.1007/s12665-021-09629-z>
45. Singh PK, Kainthola A, Singh TN (2013) Rock mass assessment along the right bank of river Sutlej, Luhri, Himachal Pradesh, India. *Geomat Nat Hazards Risk*. [doi:10.1080/19475705.2013.834486](https://doi.org/10.1080/19475705.2013.834486)
46. Singh R, Umrao RK, Singh TN (2017) Hill slope stability analysis using two and three dimension analysis: a comparative study. *J Geol Soc India*, (2017), 89(3):229–356
47. Topal T, Akin M, Ozden UA (2017) Assessment of rockfall hazard around Afyon Castle, Turkey. *Environ Geol* 53(1):191–200

48. Trivedi R, Vishal V, Pradhan SP, Singh TN, Jhanwar JC (2012) Slope stability analysis in limestone mines. *Int J Earth Sci Eng* 5(4):759–766
49. Umrao RK, Singh R, Ahmad M, Singh TN (2011) Stability analysis of cut slopes using continuous slope mass rating and kinematic analysis in Rudraprayag district. *Uttarakhand Geomaterials* 1:79–87
50. Umrao RK, Singh R, Sharma LK, Singh TN (2017) Soil slope instability along a strategic road corridor in Meghalaya, north-eastern India. *Arab J Geosci*. <https://doi.org/10.1007/s12517-017-3043-8>
51. Verma BP (1985) *Rock Mechanics for Engineers*, 1st Edition
52. Vishal V, Siddique T, Purohit R, Phophliya MK, Pradhan SP (2017) Hazard assessment in rockfall-prone Himalayan slopes National Highway-58, India: rating and simulation. *Nat Hazards* 85:487–503
53. Wyllie DC, Mah CW (2004) *Rock Slope Engineering*. Spon Press, London, p 428
54. Yoon WS, Jeong UJ, Kim JH (2002) Kinematic analysis for sliding failure of multi-faced rock slopes. *Eng Geol* 67:51–611

Figures

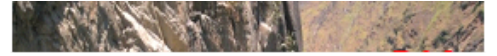
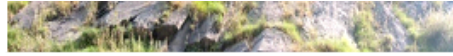
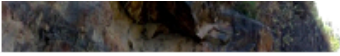


Figure 1

Location map of study area (a) Map of India, Himachal Pradesh, and District Chamba (b) Selected rock slopes along NH - 154A, Rock slopes where failure has been identified (R1, R8, R14, R10, R11, and R13)

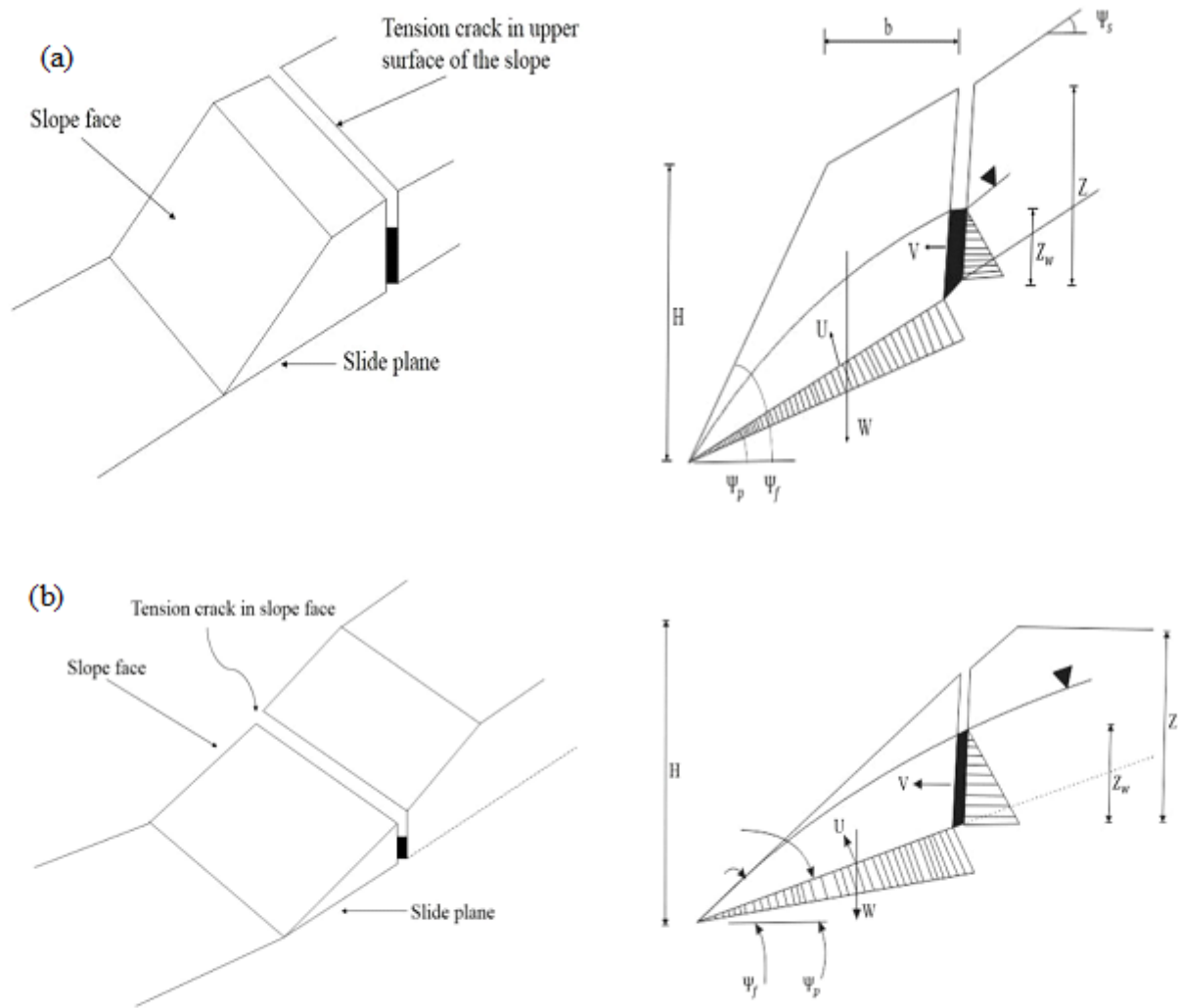


Figure 2

Geometry of slope with tension crack – Planar analysis

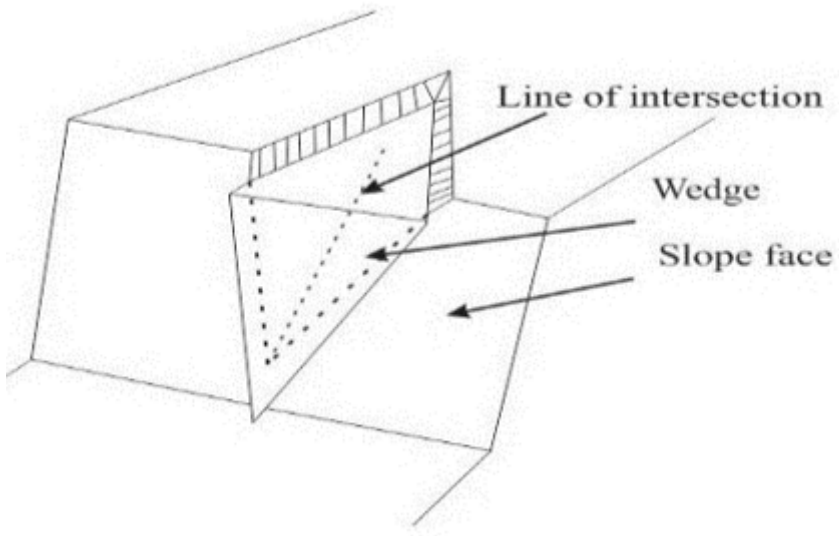


Figure 3

Wedge failure geometry

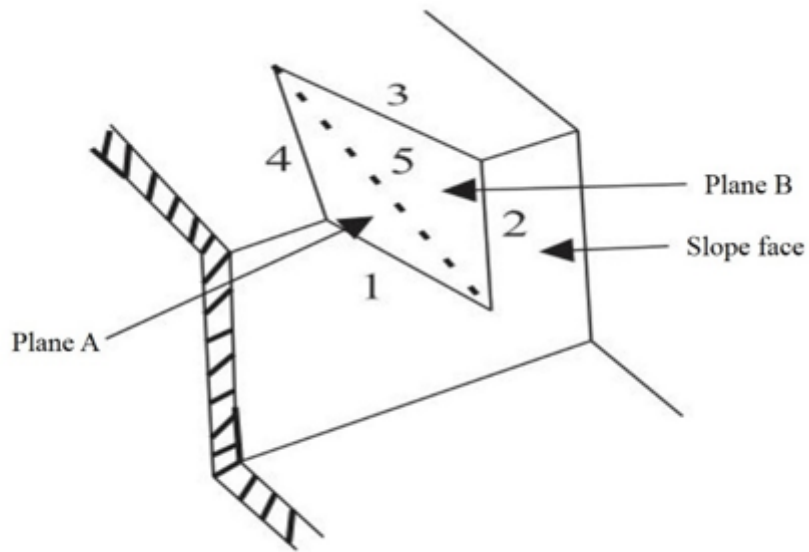


Figure 4

Geometrical representation of wedge for analyzing stability

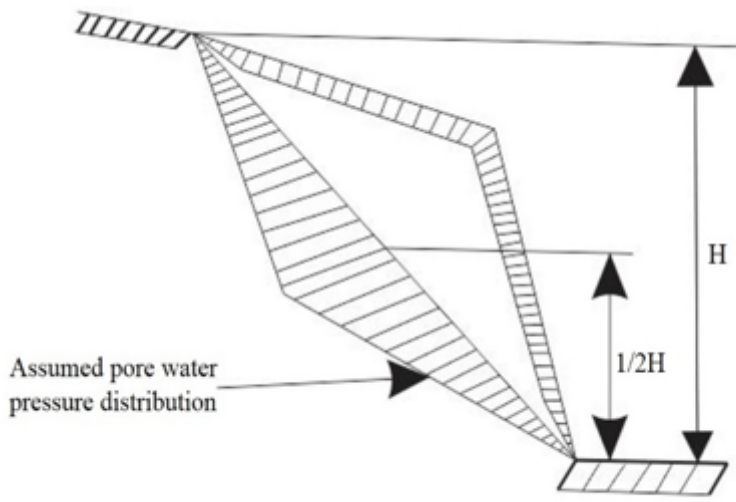


Figure 5

Geometry of wedge used for stability analysis – water pressure

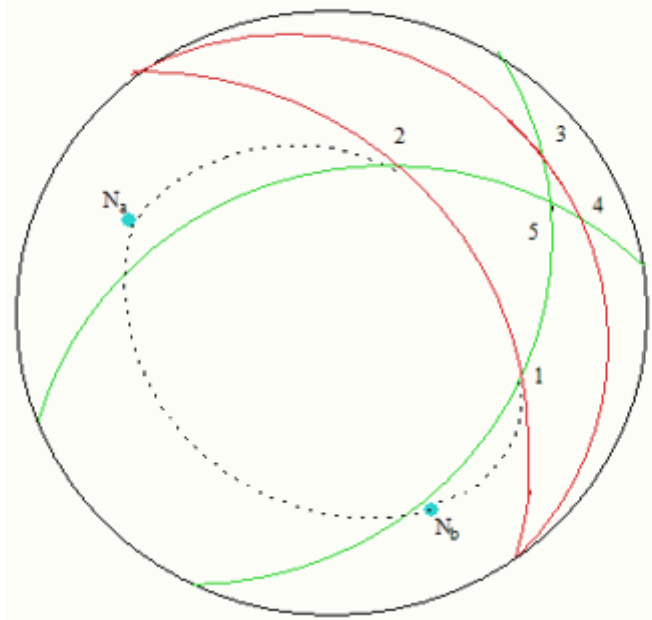
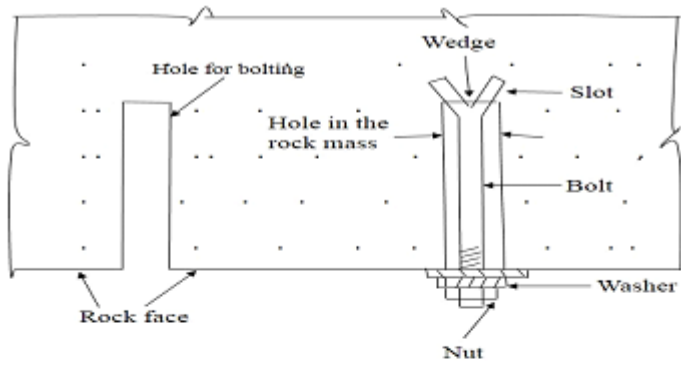


Figure 6

Stereoplot of data required for wedge stability analysis



(a)



(b)



Figure 7

Mitigation measures to prevent slope surface a) Details of rock bolting (Verma BP 1985), b) Wire mesh and anchor bolt, c) Dry-mix shotcrete process using bagged mix feeding a pump and pre-moisturizer (Wyllie and Mah 2004), d) Shotcrete-stabilized cliff (<https://en.wikipedia.org>)